# A Pattern Reconfigurable Antenna Based on $TM_{10}$ and $TM_{02}$ Modes of Rectangular Patch

**Hai-Yan Huang, Bing-Zhong Wang, Xiao Ding, and Wei Shao**

The Institute of Applied Physics
University of Electronic Science and Technology of China, Chengdu, 610054, China
haiyanhuang123@yahoo.com, bzwang@uestc.edu.cn, dx_000217@yahoo.com.cn, and
weishao@uestc.edu.cn

***Abstract*** ─ A pattern reconfigurable rectangular microstrip antenna is reported in this paper. A broadside radiation pattern and a conical pattern are obtained when it alternatively operates in the $TM_{10}$ mode and $TM_{02}$ mode of the rectangular patch. Suitable patch size parameters and feeding positions are selected so that these two modes share the same operating frequency. Two PIN diodes are employed to switch the operating modes. The configuration of the antenna is simple, which consists of a rectangular patch and a reconfigurable feeding network to excite expected mode. The feature of the proposed antenna is that the design method is explicit, based on different resonant modes with different radiation characteristics, and can be used to design other types of reconfigurable antennas.

***Index Terms*** ─ Microstrip patch, modes characteristics, and reconfigurable antenna.

## I. INTRODUCTION

Reconfigurability of an antenna refers to the capacity to adjust a radiator's characteristics in terms of resonant frequency, radiation pattern, or polarization. The dynamic tuning is achieved by manipulating a certain switching mechanism through controlling electronic, mechanical, or optical switches. Among them electronic switches are the most popular in constituting reconfigurable antennas due to their efficiency, reliability, and ease of integrating with microwave circuitry. The typical electronic switches are PIN diodes, FET transistors, and RF MEMS switches. Compared to RF MEMS switches and FET transistor, PIN diodes have acceptable performance and low price.

Pattern reconfigurable antennas are attractive in applications of surveillance and tracking, because they produce more than one radiation pattern with different directivity at the same operating frequency. In addition, manipulation of patterns is useful in avoiding noise source, mitigating electronic jamming, improving security, and increasing energy efficiency. For their attractive features, pattern reconfigurable antennas have received considerable attentions and a number of works have been demonstrated in the past years [1-3]. A typical example for pattern reconfigurable microstrip antennas is given in [4], where a Yagi–Uda antenna is selected to constitute a pattern reconfigurable antenna. By adjusting the lengths of two parasitic elements acting as the director and reflector, three reconfigurable patterns are achieved. The antenna in [5] can be regarded as a combination of a monopole and two Vivaldi slots, providing a broadside pattern and two opposite endfire patterns with a broad impedance bandwidth. The main methods to obtain a pattern reconfigurable antenna, to the authors' knowledge, are finding structures with the potential to produce pattern diversity, or reconfiguring the feeding configurations, which can be interpreted by the array theory [6].

In this paper, a new design method is presented to design reconfigurable antennas. The mode characteristics of rectangular microstrip patch are studied and applied to the pattern reconfigurable antenna design. First, the theoretical mode characteristics are analyzed. Then, a feeding network is designed according to

*Submitted On: Dec. 25, 2012*
*Accepted On: Aug. 10, 2013*

the mode characteristics. Last, a prototype antenna is fabricated and measured to verify the design concept.

## II. ANTENNA DESIGN

A microstrip antenna can be regarded as a dielectric-loaded cavity with two perfect electric conducting surfaces (top and bottom) and four perfect magnetic conducting sidewalls along its perimeter. The radiation mainly takes place at the four sidewalls of the cavity, and can be calculated by using the aperture radiating theory through introducing equivalent currents [7]. Notice that different resonant modes within the cavity have different electric field distributions at the sidewalls of the cavity, which leads to different equivalent magnetic current distributions and finally results in different radiation patterns.

Here, the $TM_{10}$ and $TM_{02}$ modes are selected to design a pattern reconfigurable antenna. Figure 1 depicts the electric field distributions and the equivalent magnetic currents of these two modes within the cavity. As shown in Fig. 1 (a) the electric field distribution of the $TM_{10}$ mode undergoes a phase reversal along the *x*-direction but is uniform along the *y*-direction. The equivalent magnetic currents along those two slots of length *L* and height *H* are of the same magnitude and the same phase. The far-zone electric fields radiated by each slot will add in phase and form a broadside pattern in the *y*-*z* plane. The same analysis procedure can be performed on the other two slots of width *W* and height *H*. Their far-zone electric fields are cancelled in the *y*-*z* plane and *x*-*z* plane. Therefore, for $TM_{10}$ mode, it possesses a broadside pattern as shown in Fig. 1 (c). The same analysis process can also be carried out for the $TM_{02}$ mode. The two slots of length *L* and height *H* are non-radiating slots. The radiating slots are those of width *W* and height *H*. Because their equivalent magnetic currents are of the same magnitude but 180° out of phase, the radiation pattern of $TM_{02}$ mode is a conical pattern in the *y*-*z* plane. Figure 1 (d) shows the pattern of $TM_{02}$ mode in the *y*-*z* plane.

Here, the $TM_{10}$ and $TM_{02}$ modes are chosen for developing a pattern reconfigurable antenna due to their attractive broadside and conical patterns. In fact, other higher modes of the rectangular patch also have similar patterns. For example, $TM_{n0}$ and $TM_{0n}$ modes, where *n* is an odd number, produce maximum radiations at broadside; on the other hand, $TM_{0m}$ and $TM_{m0}$ modes, where *m* is an even number, form nulls in the broadside direction. Theoretically, they can be used to design a pattern reconfigurable antenna. But the higher the mode, the larger the patch size will be, which goes against the antenna compactness. Except the modes mentioned above, there are other modes like $TM_{11}$ mode, which possesses a conical pattern. But if those kinds of modes are picked, it is difficult to make the two different modes resonate at the same frequency. Therefore, the operating modes used in this paper are the $TM_{10}$ and $TM_{02}$ modes.

In order to excite the desired modes, not only the operating frequency should be set close to the resonant frequency of the modes, but also the feeding positions should be properly picked. The general principle is that: first, figure out the field distributions of the modes beneath the patch; next, find those positions where the magnitudes of fields are maximum of one mode and minimum of another mode; and then place the feed lines at positions with maximum field magnitude of the desired mode and with minimum filed magnitude of the undesired mode. Through these steps the corresponding mode is efficiently and exclusively excited.

According to the electrical field distributions shown in Fig. 1 (a) and (b), when the $TM_{10}$ mode is desired, the microstrip feed lines should be placed at points B and C where the electric fields of $TM_{10}$ mode are maximum while that of $TM_{02}$ mode are minimum; when the operating mode is $TM_{02}$, the antenna is fed at point A where the electric fields of $TM_{02}$ mode are maximum while that of $TM_{10}$ mode are minimum. Figure 2 shows the simulated electric field amplitude distributions of $TM_{10}$ and $TM_{02}$ modes. It is apparent from Fig. 2 (a) that the $TM_{10}$ mode is effectively excited when the patch is fed at points B and C. Figure 2 (b) shows that the $TM_{02}$ mode is effectively excited when the patch is fed at point A.

The resonant frequency is easy to obtain by using the cavity model. The resonant frequencies of the $TM_{nm}$ modes are given by

$$f_{TM_{nm}} = \frac{1}{2\pi\sqrt{\varepsilon\mu}}\sqrt{\left(\frac{n\pi}{W}\right)^2+\left(\frac{m\pi}{L}\right)^2}\ , \qquad (1)$$

where *n* and *m* are the order of modes, and *W* and

*L* are the width and the length of the rectangular patch. It is obvious that the resonant frequency is determined by the size of the patch and the order of the modes.

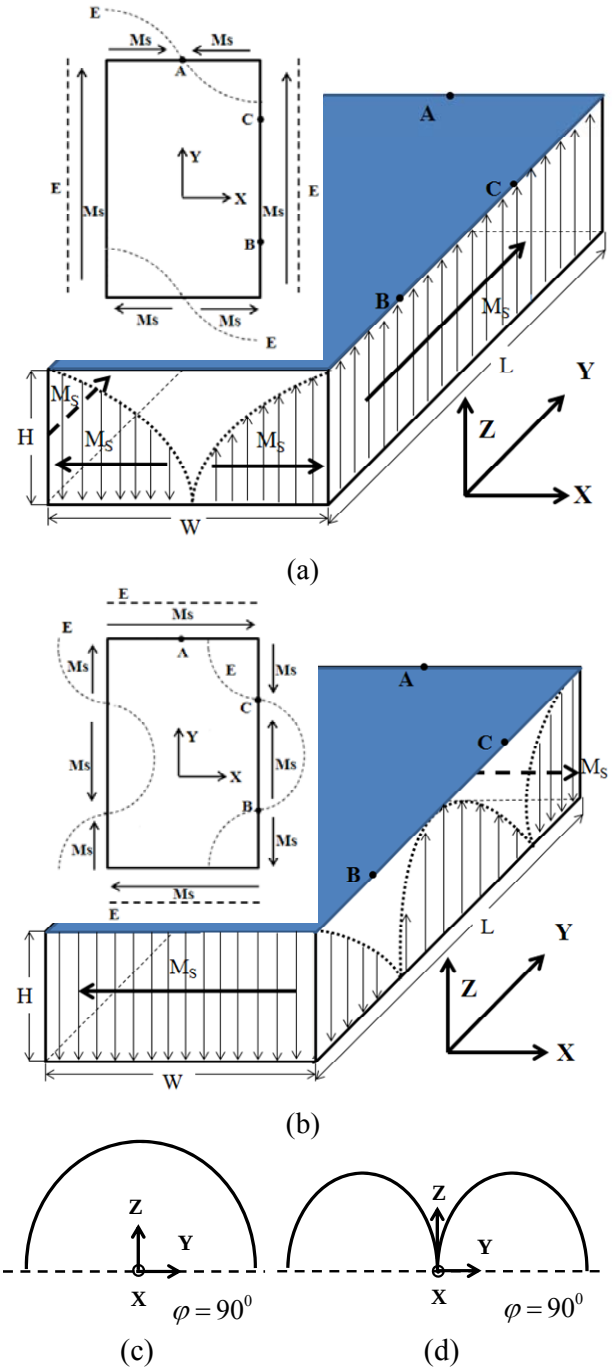


Fig. 1. Electrical field distributions: (a) $TM_{10}$ mode and (b) $TM_{02}$ mode. Radiation patterns in the *y*-*z* plane: (c) $TM_{10}$ mode and (d) $TM_{02}$ mode.

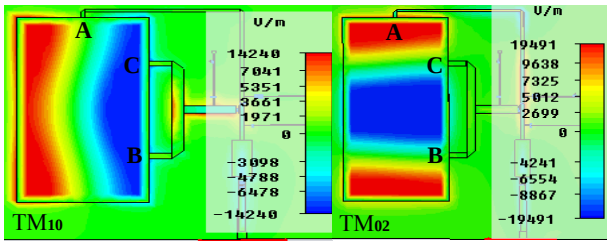


Fig. 2. Simulated electrical field amplitude distributions: (a) $TM_{10}$ mode and (b) $TM_{02}$ mode.

By carefully choosing the ratio of the length to the width, two different modes with the same resonant frequency can be obtained. In this design the ratio is chosen to be 2, so that the $TM_{10}$ and $TM_{02}$ modes share the same resonant frequency. Thus, as long as the two modes are excited alternatively, the antenna gets the capacity to provide two different radiation patterns at the same frequency.

## III. SIMULATED AND MEASURED RESULTS

To verify the reconfigurable ability of the proposed antenna, a prototype was simulated, fabricated, and measured. The antenna is printed on a substrate with a relative permittivity of 3 and a height of 1 mm. The structure of the proposed antenna is shown in Fig. 3 (a). It consists of a rectangular patch, a reconfigurable feeding network, two PIN diodes acting as switches and a simple bias network providing DC bias to the PIN diodes. There are two gaps of width 0.5 mm in the feeding network, across which the PIN diodes are mounted using electrically conductive silver epoxy. In this paper, the implemented diodes are beam lead PIN diodes (MA4AGBL912). According to the PIN diode datasheet [8], the diode has a forward resistance of typical value 4 Ω for the ON state while a parallel circuit with a capacitance of 0.025 pF and a resistance about 4 K Ω for the OFF state. The circuit schematic of the bias network for the antenna is shown in Fig. 3 (b), where capacitor C1 is the DC blocking capacitor, inductor L2 is the RF chock inductor, and capacitor C2 is the filter capacitor, which forms a low-pass filter with the inductor L1 for a better isolation from the RF signals.

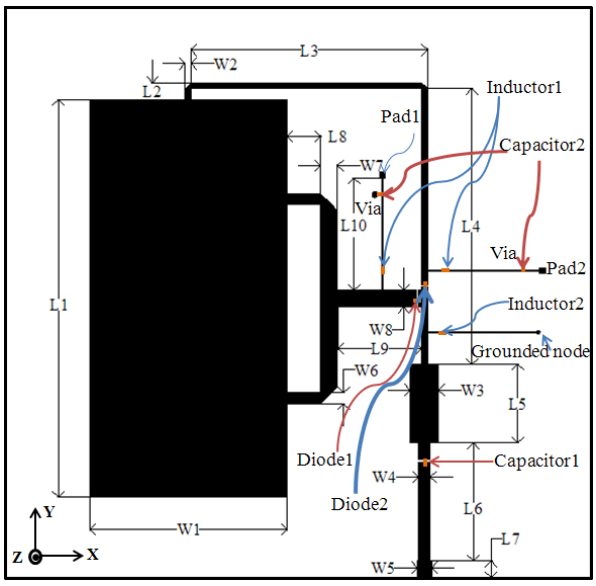


(a)

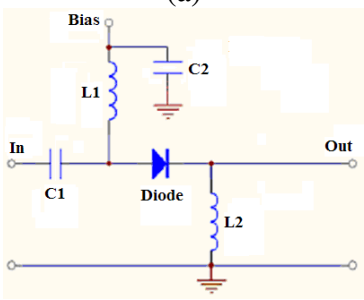


(b)

Fig. 3. (a) Structure of the reconfigurable rectangular patch and (b) circuit schematic of the DC bias network.

In the practical design, two chip capacitors of capacitance 20 pF labeled as Capacitor 2 in Fig. 3 (a) and two chip inductors of inductance 100 nH labeled as Inductor 1 in Fig. 3 (a) are employed to build the low-pass filters with a rejection band starting from 0.5 GHz, which is much lower than the operating frequency 2.45 GHz, to ensure the isolation from the RF signals. A chip inductor of inductance 100 nH, labeled as Inductor 2 in Fig. 3 (a), is mounted on the grounded high impedance line. A chip capacitor with capacitance 10 pF, labeled as Capacitor 1 in Fig. 3 (a), is employed to prevent the DC bias voltage flowing into RF source at the antenna terminal. Because the applied diodes (MA4AGBL912) can also work in the OFF state when the bias is 0 V according to its datasheet [8], there is only one grounded line required. When positive bias voltage is provided for Diode 1 and no bias voltage for Diode 2, Diode 1 is in the ON state and Diode 2 is in the OFF state, and vice versa. When Diode 1 is ON and Diode 2 is OFF, the patch is fed at points B and C as shown in Fig. 2 (a). The $TM_{10}$ mode is excited and the antenna radiates a broadside pattern. On the contrary, when Diode 1 is OFF and Diode 2 is ON, the patch is fed at the point A and the $TM_{02}$ mode is excited as shown in Fig. 2 (b). In this case the radiation pattern is conical.

The parameters of the antenna are provided in Table I. Since microstrip antennas are resonant antennas, the length and width of the patch are important design parameters, which greatly affect resonant frequency and input impedance. In this paper, the proposed antenna operates at 2.45 GHz. In order to make the two modes work at the same frequency, the length and the width of the patch are chosen to be 70.7 mm and 35.2 mm, respectively. The ratio of the length to the width is not exactly equal to 2. The slight deviation is due to the small adjustment of length for achieving a better impedance match.

Table I: Dimensions of the proposed antenna (in unit of millimeter).

| | | | | | |
|---|---|---|---|---|---|
| W1 | 35.2 | W2 | 1 | W3 | 5 |
| W4 | 2 | W5 | 2.5 | W6 | 2 |
| W7 | 3 | W8 | 3 | L1 | 70.7 |
| L2 | 3 | L3 | 42.1 | L4 | 49 |
| L5 | 14 | L6 | 21 | L7 | 3 |
| L8 | 6 | L9 | 15 | L10 | 20 |

The antenna is analyzed by the time domain solver of CST Microwave Studio. Figure 4 gives the simulated surface electric current distributions. As depicted in Fig. 4 (a), for the $TM_{10}$ mode, the surface current vectors are in the *x*-direction and the maximum takes place along the *y*-direction center line of the patch. For the $TM_{02}$ mode, as demonstrated in Fig. 4 (b), the surface current vectors are in the *y*-direction, and the two parts of the surface current distribution are 180° out of phase, which accounts for a radiation pattern with a null at broadside. Figure 5 exhibits the simulated 3-D radiation patterns of the proposed antenna. As shown in Fig. 5 (a), the pattern of mode $TM_{10}$ is a typical broadside pattern in the *y*-*z* plane. It is obvious that the pattern of $TM_{02}$ mode is a conical pattern with a null at broadside in the *y*-*z* plane.

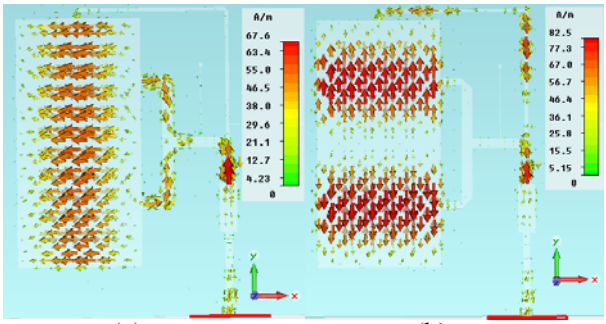

(a) (b)

Fig. 4. Surface current distributions of the proposed antenna: (a) $TM_{10}$ mode when diode 1 is ON and diode 2 is OFF and (b) $TM_{02}$ mode when diode 1 is OFF and diode 2 is ON.

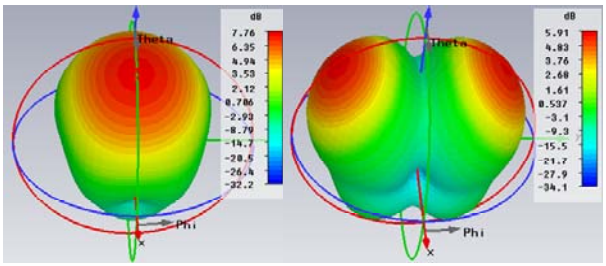

(a) (b)

Fig. 5. 3-D radiation patterns of the proposed antenna: (a) $TM_{10}$ mode and (b) $TM_{02}$ mode.

The input reflection coefficient measurements are done by using an Agilent's E8361A network analyzer. The simulated and measured reflection coefficients of the $TM_{10}$ and $TM_{02}$ modes are given in Fig. 6. The impedance bandwidths of the $TM_{10}$ mode and the $TM_{02}$ mode are relatively narrow compared to commonly used antennas. One reason is that the impedance bandwidth of a microstrip antenna is inherently narrow. This is due to the fact that microstrip antennas are resonant antennas. The input impedance of a microstrip antenna is found to vary fast with frequency, and this feature limits the frequency range over which it can be matched to its feed line. Although some bandwidth expanding techniques are widely used to enlarge its impedance bandwidth, such as cutting slots on the patch and using proximity coupling or aperture coupling, those bandwidth expanding methods can not be utilized here, because those approaches usually use more than one mode of the patch, which may cause distortion in the radiation pattern. Figure 6 (a) shows that the measured and simulated return losses are in an acceptable agreement, and the resonant frequencies are exactly at the designed 2.45 GHz. Figure 6 (b) shows that, for the $TM_{02}$ mode, the measured resonant frequency shifts slightly to the higher frequency. This discrepancy between the measured and simulated results can be attributed to the inaccuracies in the fabrication process, the variation in discrete component parameters from values given in manufacturer's data sheet, and diode parasitic parameters, which are not considered in simulation procedure. The shift, since it is very small, does not considerably affect the performance of the antenna.

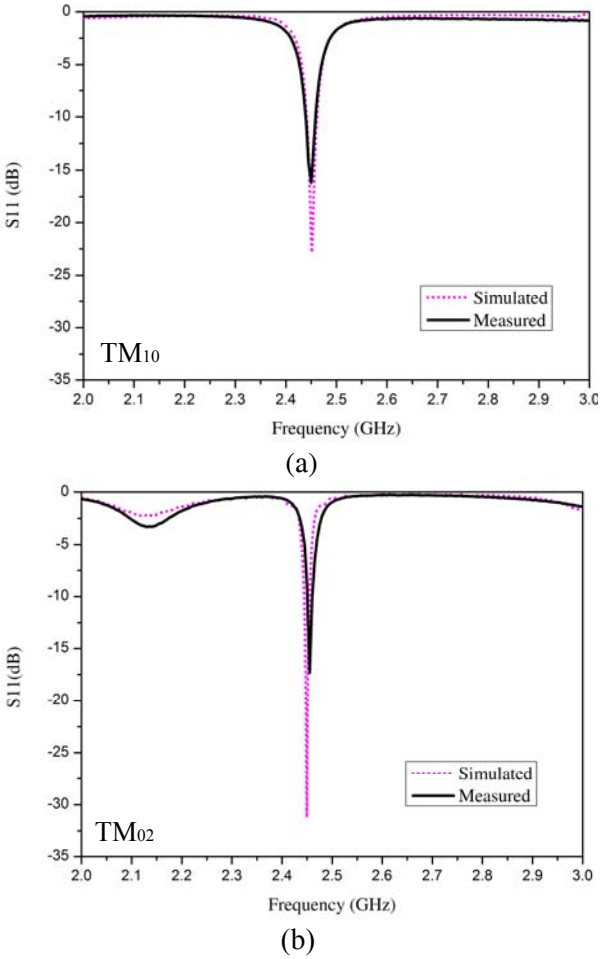


Fig. 6. Simulated and measured input reflection coefficients: (a) $TM_{10}$ mode and (b) $TM_{02}$ mode.

Figure 7 (a) is the photograph of the fabricated antenna with the mounted lump elements. Radiation patterns are measured for the $TM_{10}$ and $TM_{02}$ modes using a spherical near-field

measurement system as shown in Fig. 7 (b). The orientations of the coordinate system used in all radiation pattern figures are the same as the one shown in Fig. 3 (a). Simulated and measured radiation patterns of the two modes are compared in the *y*-*z* and the *x*-*z* planes, and the *y*-*z* plane is the principle plane where pattern diversity takes place.

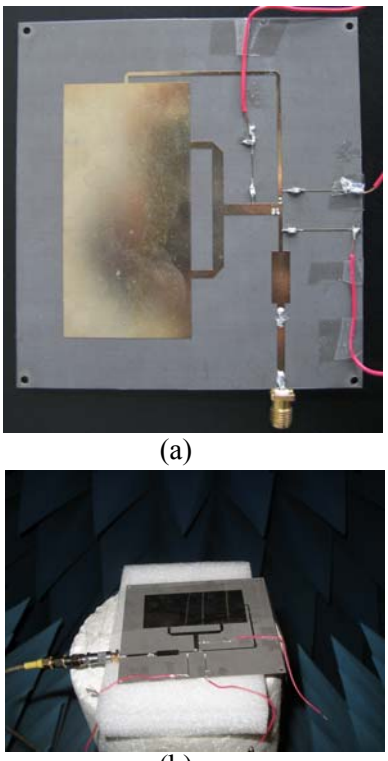

(a)

(b)

Fig. 7. (a) Photograph of the fabricated antenna and (b) photograph of the proposed antenna in a spherical near-field measurement system.

As shown in Fig. 8 (a), well-defined broad radiation pattern can be observed in the *y*-*z* plane for the $TM_{10}$ mode. The simulated and measured maximum radiation gains are 6.6 dBi and 5.7 dBi, respectively. Both simulated and measured half-power beamwidths are $64^0$. The cross polarization, which mainly comes from the $TM_{02}$ mode, is lower than -12 dBi for the measured result.

Figure 8 (b) shows that it is a conical radiation pattern for the $TM_{02}$ mode in the *y*-*z* plane. The beam peaks of the measured conical pattern point at $\pm$ $40^0$. The measured half-power beamwidth is $53^0$. The maximum radiation gains are 5.7 dBi and 3.8 dBi for simulation and measurement, respectively. The measured maximum gain is 1.9 dBi smaller than the simulated result. One reason for this phenomenon is that the resonant frequency of the $TM_{02}$ mode shifts a little bit from the designed 2.45 GHz to the higher frequency, which makes the reflection coefficient larger than -10 dB at the operating frequency and results in the degradation of the gain. The cross polarization, which mainly comes from the $TM_{10}$, is lower than -11 dBi for the measured result. By comparing Fig. 8 (a) with Fig. 8 (b), it can be found that the gain of the $TM_{10}$ mode is higher than that of the $TM_{02}$ mode. This is due to the fact that conical radiation pattern disperses radiation energy. It also can be found that the cross polarization of the $TM_{02}$ mode is higher than that of the $TM_{10}$ mode, which reveals that even though the designed resonant frequencies are the same, the $TM_{10}$ mode is stronger than the $TM_{02}$ mode and is harder to be suppressed.

Figure 8 (c) shows the radiation patterns of the $TM_{10}$ mode in the *x*-*z* plane. From Fig. 8 (c) it can be seen that there is a tilt of the maximum radiation, which pushes the maximum radiation to the +*x*-direction. The main factor which accounts for this phenomenon is the spurious radiation of the feed lines. The 3-D radiation pattern in Fig. 5 (a) gives a more intuitive view. The feeding network placed beside the patch plays a role as a director, which drags the radiation pattern from the broadside to the +*x*-direction in the *x*-*z* plane. The distortion of the radiation pattern can be alleviated considerably by using other feeding techniques such as probe feeding and aperture coupling. However, those techniques are not used here, because for the probe feeding it is not convenient to integrate switches with the feeding networks; and for the aperture coupling, it usually excites multiple modes and it is hard to separate them. Furthermore, since the pattern reconfigurable ability is designed in the *y*-*z* plane, except for the maximum gain undergoing a 1.1 dBi decrease, the tilt of pattern in the *x*-*z* plane does not significantly influence the performance of the antenna.

Figure 8 (d) shows the radiation patterns of the $TM_{02}$ mode in the *x*-*z* plane, which indicates that the radiation of $TM_{02}$ mode in the *x*-*z* plane is small. This is due to the fact that the pattern of $TM_{02}$ mode possesses a theoretical null in the broadside direction. It can be found clearly in the

simulated 3-D pattern as shown in Fig. 5 (b). In general, the agreements between the simulated and the measured results are acceptable, and the performances of the proposed antenna confirm the feasibility of the design concept.

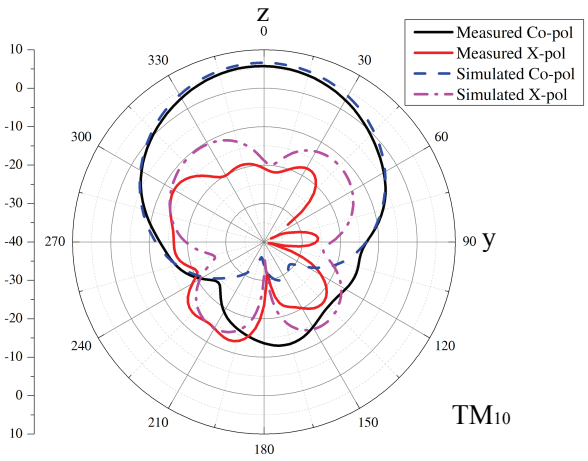


(a)

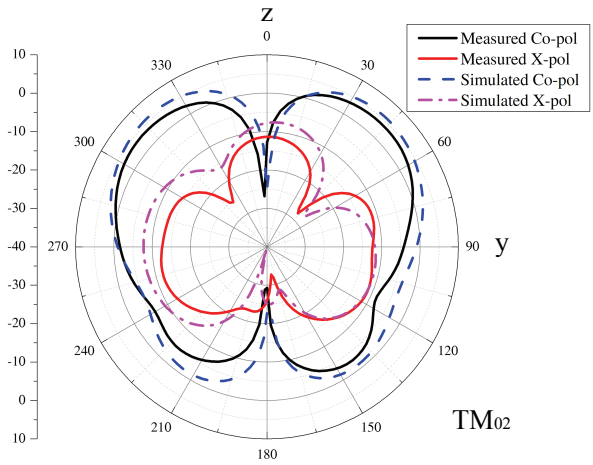


(b)

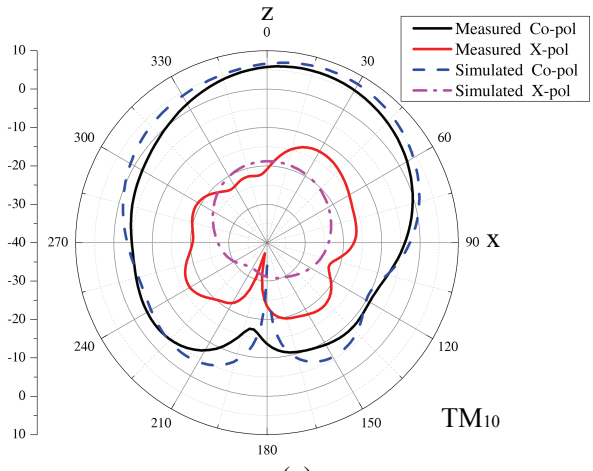


(c)

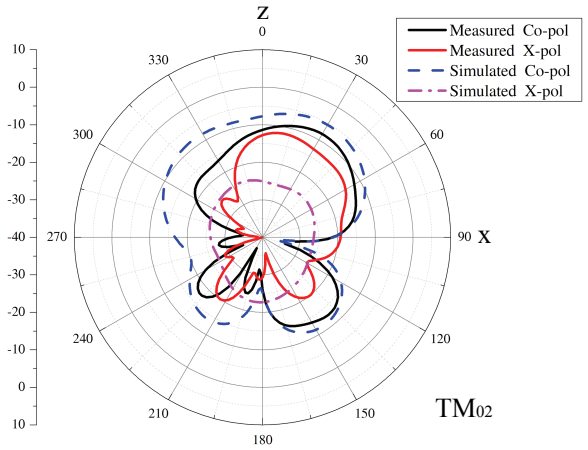


(d)

Fig. 8. Simulated and measured radiation patterns at 2.45 GHz: (a) $TM_{10}$ mode in the *y-z* plane, (b) $TM_{02}$ mode in the *y-z* plane, (c) $TM_{10}$ mode in the *x-z* plane, and (d) $TM_{02}$ mode in the *x-z* plane.

Figure 9 gives the simulated and measured gains of the proposed antenna versus frequency. The proposed antenna is a narrow-band antenna, which is due to the realization of operating in $TM_{10}$ and $TM_{02}$ modes at the same frequency. The frequency band for gain investigation is set from 2.43 GHz to 2.47 GHz. From Fig. 9, it can be seen that the measured gain varies from 4.9 dBi to 6.8 dBi for $TM_{10}$ mode, while the simulated gain varies from 5.2 dBi to 7.6 dBi for $TM_{10}$ mode; and that the measured gain varies from 0.3 dBi to 4.1 dBi for $TM_{02}$ mode, while the simulated gain varies from 0.5 dBi to 5.7 dBi for $TM_{02}$ mode. Owing to the narrow operating band, gain changes considerably with frequency especially for $TM_{02}$ mode. The maximum measured gain of $TM_{02}$ mode is at 2.46 GHz, just like the measured $S_{11}$ of $TM_{02}$ mode shifts slightly towards higher frequency as shown in Fig. 6 (b).

## IV. CONCLUSION

A pattern reconfigurable rectangular patch antenna operating at the $TM_{10}$ mode or the $TM_{02}$ mode is presented in this paper. PIN diodes are used to alter the feeding positions, and to steer the operating modes. The theory and experiments presented in this work show that this simple rectangular patch antenna can provide a broadside pattern or a conical pattern at 2.45 GHz. The main limitation of this antenna is its narrow impedance

bandwidth, which needs to be improved in the future. The design method can be used in other shapes of microstrip antennas for reconfigurable antenna designs. For example, circular patches and annular rings, the high order modes of which also possess conical patterns, can be used to design similar pattern reconfigurable antennas. This antenna can be used in wireless systems in which we are not much concerned about the polarization while the direction of arrival is a big concern.

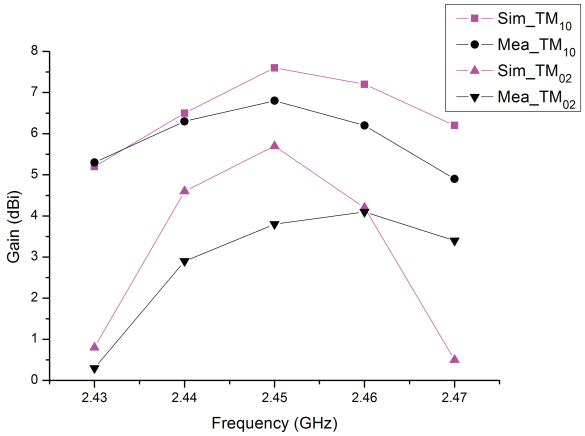


Fig. 9. Simulated and measured gains of the proposed antenna versus frequency.

## REFERENCES

[1] X. -S. Yang, B. -Z. Wang, and W. Wu, "Yagi patch antenna with dual-band and pattern recofigurable characteristic," *IEEE Antennas Wireless Propagat. Lett.*, vol. 6, pp. 168-171, 2007.

[2] Y. -Y. Bai, S. Xiao, and B. -Z. Wang, "Two-dimensional pattern scanning by linear phased array with pattern reconfigurable elements," *Applied Computational Electromagnetics Society (ACES) Journal*, vol. 25, no. 2, pp. 144-148, Feb. 2010.

[3] S. Xiao, Y. -Y. Bai, and B. -Z. Wang, "Scan angle extension by array with pattern reconfigurable elements," *Applied Computational Electromagnetics Society (ACES) Journal*, vol. 24, no. 5, pp. 453-457, Oct. 2009.

[4] S. Zhang, G. H. Huff, J. Feng, and J. T. Bernhard, "A pattern reconfigurable microstrip parasitic array," *IEEE Trans. Antennas Propagat.*, vol. 52, pp. 2773-2776, 2004.

[5] G. M. Zhang, J. S. Hong, B. -Z. Wang, G. Song, and P. Li, "Design and time-domain analysis for a novel pattern reconfigurable antenna," *IEEE Antennas Wireless Propagat. Lett.*, vol. 10, pp. 365-368, 2011.

[6] W. Cao, B. Zhang, A. Liu, T. Yu, D. Guo, and K. Pan, "A reconfigurable microstrip antenna with radiation pattern selectivity and polarization diversity," *IEEE Antennas Wireless Propagat. Lett.*, vol. 11, pp. 453-456, 2012.

[7] C. A. Balanis, *Antenna Theory, Analysis and Design*, John Wiley and Sons, USA, 2005.

[8] MA4AGBLP912, M/A-COM Technology Solution Inc. www.macomtech.com